Journal Name

ARTICLE TYPE

Cite this: DOI: 00.0000/xxxxxxxxxx

Supporting Information

1 Length Defect Estimate

Let's suppose a curve in space is driven by a vector $\vec{r}^*$ which is described by its parameter t, or $\vec{r}^*(t) = x^*(t)\hat{i} + y^*(t)\hat{j} + z^*(t)\hat{k}$. If the curve parametrization in function of t is known, then its length C^* from a point A to B is given by

$$C^* = \int_A^B \left| \frac{\mathrm{d}\vec{r}^*}{\mathrm{d}t} \right| \mathrm{d}t \tag{1}$$

The curve made by the twisted loop defect is very similar to a path created on the surface of a sphere when it crosses the meridians with a fixed angle, also known as loxodromic curve. Considering the condition that z^* has maximum value when $x^* = y^* = 0$, the rhumb line describing the single-twisted ring defect containing M isocline lines crossing a bipolar axis of a sphere with radius $R^*_{\mathrm{lox}} (= R_{\mathrm{lox}}/\Lambda)$ can be parametrized as

$$\begin{cases} x^*(t) &= R^*_{\mathrm{lox}}(-1)^{k+1}\sin(t)\sin\left((M+1)t\right) \\ y^*(t) &= R^*_{\mathrm{lox}}(-1)^{k}\sin(t)\cos\left((M+1)t\right) \qquad 0 \le t \le \pi,\ k = 1,2 \\ z^*(t) &= R^*_{\mathrm{lox}}\cos(t) \end{cases} \tag{2}$$

The parameter $k = 1$ describes half of the complete curve, while $k = 2$ refers to the other one. As the loxodrome is regular, it is enough to integrate over half of the curve, since the other part has the same length. So, for $k = 1$, and considering integer values of $M > 0$, the estimate for the total scaled length of twisted loop defect C^*_{loop}, according to Eqs. (1) and (2), can be written as

$$C^*_{\mathrm{loop}}(M) = 2R^*_{\mathrm{lox}} \int_0^{\pi} \sqrt{1 + (M+1)^2 \sin^2(t)}\ \mathrm{d}t \tag{3}$$

2 Results

2.1 Achiral sample – N = 0

For the purpose of examining the thermal quench simulations, we discussing the non-chiral case, $N = 0$, which implies $\sigma^* = 0$. As $T^i_R < T^{IN}_R$, and starting from a random state, there is a natural trend of alignment which favors the nematic phase so that in few cycles, compared to the whole range of simulations, the expected nematic structure takes place showing the known patterns in the literature both for H and PD anchoring. In Figure SI 1 we show results for CCN-37 sample in (a) H and (b) PD anchoring, both with $J_s = 1.00$ at $T_R = 0.100$ (200 kMCs). The directors are colored according to the order parameter S, so regions in blue tones are near defects where the spins suffer abrupt changes in the direction while orange tones are regions of high ordination. The Müller textures are shown for Ci and Li polarized light while in a transparent blue sphere representing the LC droplet, we plot red isosurfaces of order parameter $S = 0.74$ to see how the defects are arranged in the bulk.

In the H case, the hedgehog pattern appears since the surface energy overlaps the bulk energy, so the directors align in the radial direction, as shown in Figure SI 1(a). Due to the stochastic features in the simulations, it is difficult to exactly obtain a point defect located in the middle of the lattice. Instead, we observe a short-length ring defect oscillating in the center of the droplet. As the ring can be considered a regular circle with a radius near 2 sites, its scaled length C^* is around 4π. The Müller textures in Figure SI 1(a) show regular circles of minimum intensity for Ci polarized light, while for the Li one appears an alternating pattern of dark and bright brushes, similar to experiments.[1–10] The directors are radially aligned and the polarizers are crossed, so brushes maximum and minimum intensities oscillate each 45°.

When the anchoring is PD, shown in Figure SI 1(b), the sample shows the formation of BS with two antipodal boojums appearing on the droplet's surface, as expected by the Poincaré-Hopf theorem. The boojums have topological charge $s = +1$ and are indicated by the blue arrows. The directors in the bulk follow imaginary lines similar to electric field lines created by two opposite charges, and the bend distortion propagates near the surface while the splay distortion surrounds the defects. This resulting structure is cylindrically symmetric around the bipolar axis connecting the boojums and textures show flat elliptical rings with the longer axis perpendicular to the bipolar axis[5,7,9–11]. These elliptical dark brush rings are formed due to the total optical retardation effect, since the transmittance, or light intensity, is proportional to $\sin^2\left(\pi\Delta L/\lambda^{'}\right)$ with $\Delta L = \int_{-R}^{R} \Delta n\ \mathrm{d}l$, where l is the axis parallel to the light propagation[11], and $\Delta n = n_e - n_o$. So, dark regions appear for $\Delta L/\lambda^{'} = m$ with m integer.

Even setting weak anchoring energy with $J_s = 0.25$ for the H case, the CCN-37 sample presents the same described behavior. Also, simulations for OCA show the same results for both moderate H and PD anchoring, and for the weak H anchoring case.

[a] Department of Physics – Maringá State University, Avenida Colombo 5790, Maringá (PR), Brazil.
[b] Department of Physics – Federal Technological University of Paraná, Rua Marcílio Dias, 635, Apucarana (PR), Brazil.
‡ E-mail: rzola@utfpr.edu.br

† Electronic Supplementary Information (ESI) available: [details of any supplementary information available should be included here]. See DOI: 00.0000/00000000.

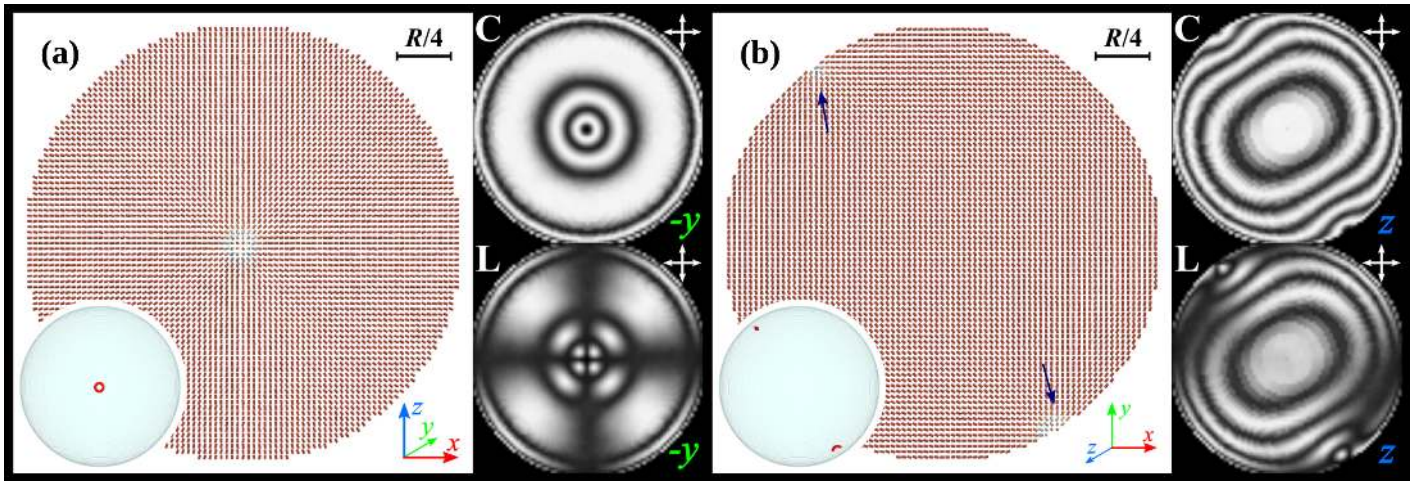

Fig. SI 1 Simulations for CCN-37 sample with $N = 0$ (nematic sample) in moderate $J_s = 1.00$ (a) H anchoring, and (b) PD anchoring. In both cases, $T_R = 0.100$ (200 kMCs). The isosurfaces were built with $S = 0.74$ as the threshold. The director field color is scaled by the value of S with blue and orange tones for low and high ordination regions, respectively. Müller matrix represents the Ci and the Li polarized light passing through the droplet. (a) The directors align radially and a small ring defect is formed in the center of the droplet, arranging in the hedgehog pattern. The linearly polarized light texture shows crossed isogyres characteristic of the radially aligned droplet. (b) The BS takes place over the bulk and two boojums with topological charge $s = +1$ are localized diametrically opposed, which satisfies the Poincaré-Hopf theorem. Near the boojums, highlighted by the blue arrows, the sample suffers an accentuated splay distortion. Apart from boojums, textures show alternative maximum and minimum light intensity in flat elliptical shapes.

Notes and references

1 O. D. Lavrentovich and E. M. Terent'ev, *Zh. Eksp. Teor. Fiz.*, 1986, **91**, 2084–2096.

2 E. Brasselet, N. Murazawa, S. Juodkazis and H. Misawa, *Phys. Rev. E*, 2008, **77**, 041704.

3 M. Humar, M. Ravnik, S. Pajk and I. Muševič, *Nat. Photonics*, 2009, **3**, 595.

4 S. Sivakumar, K. L. Wark, J. K. Gupta, N. L. Abbott and F. Caruso, *Adv. Funct. Mater.*, 2009, **19**, 2260–2265.

5 I.-H. Lin, D. S. Miller, P. J. Bertics, C. J. Murphy, J. J. de Pablo and N. L. Abbott, *Science*, 2011, **332**, 1297–1300.

6 D. S. Miller, X. Wang, J. Buchen, O. D. Lavrentovich and N. L. Abbott, *Anal. Chem.*, 2013, **85**, 10296–10303.

7 L. N. Tan, G. J. Wiepz, D. S. Miller, E. V. Shusta and N. L. Abbott, *Analyst*, 2014, **139**, 2386–2396.

8 M. Humar, *Liq. Cryst.*, 2016, **43**, 1937–1950.

9 A. V. Dubtsov, S. V. Pasechnik, D. V. Shmeliova, A. S. Saidgaziev, E. Gongadze, A. Iglič and S. Kralj, *Soft Matter*, 2018, **14**, 9619–9630.

10 A. Eremin, H. Nádasi, M. Kurochkina, O. Haba, K. Yonetake and H. Takezoe, *Langmuir*, 2018, **34**, 14519–14527.

11 J. Jiang and D.-K. Yang, *Liq Cryst.*, 2018, **45**, 102–111.